nature materials

ARTICLES

PUBLISHED ONLINE: 27 JULY 2015 | DOI: 10.1038/NMAT4355

A pH-responsive supramolecular polymer gel as an enteric elastomer for use in gastric devices

Shiyi Zhang[1], Andrew M. Bellinger[1,2], Dean L. Glettig[1], Ross Barman[1,3], Young-Ah Lucy Lee[1], Jiahua Zhu[4], Cody Cleveland[1], Veronica A. Montgomery[1], Li Gu[1], Landon D. Nash[5], Duncan J. Maitland[5], Robert Langer[1,6]* and Giovanni Traverso[1,3]*

Devices resident in the stomach—used for a variety of clinical applications including nutritional modulation for bariatrics, ingestible electronics for diagnosis and monitoring, and gastric-retentive dosage forms for prolonged drug delivery—typically incorporate elastic polymers to compress the devices during delivery through the oesophagus and other narrow orifices in the digestive system. However, in the event of accidental device fracture or migration, the non-degradable nature of these materials risks intestinal obstruction. Here, we show that an elastic, pH-responsive supramolecular gel remains stable and elastic in the acidic environment of the stomach but can be dissolved in the neutral-pH environment of the small and large intestines. In a large animal model, prototype devices with these materials as the key component demonstrated prolonged gastric retention and safe passage. These enteric elastomers should increase the safety profile for a wide range of gastric-retentive devices.

Interest in the development of gastric-resident and gastric-retentive devices has been increasing owing to their broad applications, including bariatric interventions for nutritional modulation to address the global obesity epidemic[1–3], ingestible electronics for real-time physiological monitoring and improving patient health[4–7], and daily dosage forms for prolonged oral drug delivery[8–12]. To achieve prolonged retention in the gastric cavity without exiting through the pylorus (diameter ~ 1.3 cm; refs 13,14), gastric devices are often designed to expand to greater than 2 cm in diameter. At the same time, to ensure the safe delivery of large objects through the narrow oesophagus (diameter 1.5–2 cm; ref. 15), those gastric devices are often made—at least in part—of elastic polymers for compacting or folding whole devices into smaller configurations[16]. Unfortunately, owing to the non-degradable or non-dissociable nature of elastic polymers, those large-sized devices can cause complications, such as intestinal obstruction after the migration of fractured components or even whole devices, requiring surgical intervention for removal[17–21]. These complications have been observed across a range of devices, including ingestible electronic devices[18] and percutaneous feeding tubes[19], as well as intragastric balloons for weight loss[20,21]. In spite of the broad and increasing clinical utility of these devices as extended retention systems[22], there is one striking omission in their functions: a mechanism to prevent intestinal obstruction on exiting the stomach.

Given the significant pH difference between the gastric (pH 1–3) and intestinal (pH ~ 6.8) environments, we envisage that a pH-responsive elastomer that is stable in acidic conditions but dissolvable in neutral or alkaline conditions may address this unmet clinical need. Enteric polymers have been previously developed and are generally used as coatings of oral pills and capsules to protect the active pharmaceutical ingredients from the high acidity in the gastric environment[23,24]. These materials share a common structure by having a large hydrophobic moiety and carboxyl groups for pH responsiveness. Existing enteric polymers are generally rigid, and often brittle, and therefore have not found utility in the application of gastric-retentive devices so far. Combining elastic and enteric properties remains a great challenge for material development. Recent advances in supramolecular polymer gels[25,26] present many examples of materials with tunable mechanical properties and various environmental stimuli-responsiveness[27–31]. For instance, a family of supramolecular polymer gels that is loosely crosslinked by static interactions, and possesses good elasticity and stimuli-responsiveness to a NaCl solution, which in turn disrupts the charge–charge interactions[32]. Although studies on supramolecular polymer gels and responsive polymers have enriched our knowledge towards polymeric materials, only a few applications taking advantage of their unique properties have been demonstrated[33,34]. We predicted that a supramolecular polymer gel, which is physically crosslinked by hydrogen bonds between carboxyl groups, could have good elasticity and also be enteric for next-generation gastric devices, enabling dissolution of devices into components that can pass through the gastrointestinal tract.

Here, we describe the first material combining both elastic and enteric properties, allowing the construction of gastric devices with facile delivery, prolonged gastric retention, and an improved safety profile. The material is a unique supramolecular polymer gel with elastic properties in acidic environments, and that dissolves in water under neutral conditions. Using this enteric elastomer (EE) as the key component, we built a variety of prototype gastric-resident devices that showed, in a large animal model, prolonged gastric retention (two to seven days) after delivery via administration of an encapsulated device or endoscopic placement of the

[1]Department of Chemical Engineering and Koch Institute for Integrative Cancer Research, Massachusetts Institute of Technology, Cambridge, Massachusetts 02139, USA. [2]Cardiovascular Division, Department of Medicine, Brigham and Women's Hospital, Harvard Medical School, Boston, Massachusetts 02115, USA. [3]Division of Gastroenterology, Massachusetts General Hospital, Harvard Medical School, Boston, Massachusetts 02114, USA. [4]Center for Nanophase Materials Sciences, Oak Ridge National Laboratory, Oak Ridge, Tennessee 37831, USA. [5]Department of Biomedical Engineering, Biomedical Device Laboratory, Texas A&M University, College Station, Texas 77843, USA. [6]Harvard–MIT Division of Health Sciences and Technology, Massachusetts Institute of Technology, Cambridge, Massachusetts 02139, USA. *e-mail: rlanger@mit.edu; ctraverso@partners.org

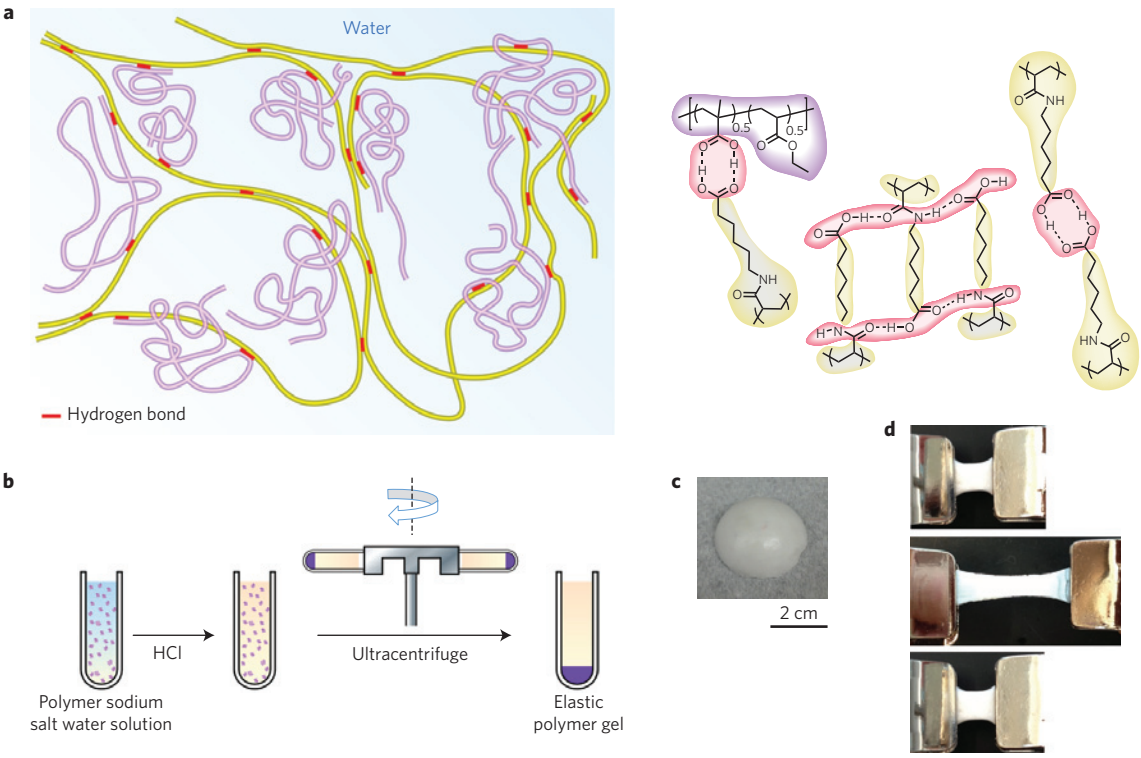

Figure 1 | Schematic representation, manufacturing and macroscopic characteristics of the enteric elastomer. a, Proposed supramolecular polymer gel network. Structures in yellow, synthesized poly(acryloyl 6-aminocaproic acid) (PA6ACA, M_n = 61,600–112,700, M_w = 347,300–466,300); structures in purple, linear poly(methacrylic acid-co-ethyl acrylate) (EUDRAGIT L 100-55, M_n = 72,300, M_w = 241,000); red part, inter-polymer hydrogen bonds. **b**, Manufacturing process of the polymer gel. Left, the homogeneous solution of PA6ACA sodium salt solution and L 100-55 sodium salt solution with varying polymer weight ratios. Middle, the addition of HCl solution resulting in precipitation. Right, formation of the elastic polymer gel after ultracentrifugation. **c**, Photo of a piece of the polymer gel obtained after ultracentrifugation. **d**, Images of stretch and recovery testing of a polymer gel with PA6ACA:L 100-55 = 1:2. Top, 1.5 cm piece of polymer gel held between two clamps. Middle, stretching of the polymer gel to three times its initial length. Bottom, recovery of the polymer gel 5 min after the external force was removed. Scale bar is 2 cm for **c** and **d**.

device in the stomach, and subsequent safe passage through the lower gastrointestinal tract on dissociation. Although there have been extensive studies and commercial examples of gastric-retentive devices since the 1970s (refs 9,35), this manuscript presents the first demonstration of both extremely prolonged gastric retention and safe gastrointestinal passage with the help of this innovative combination of elastic and enteric properties contained in one material.

Preparation of the polymer gel as an enteric elastomer (EE)

Figure 1 depicts the proposed supramolecular network structure of the EE polymer gel. The EE consists of two synthetic macromolecules, poly(acryloyl 6-aminocaproic acid) (PA6ACA, Supplementary Scheme S1) and poly(methacrylic acid-co-ethyl acrylate) (EUDRAGIT L 100-55). L 100-55 is a pharmaceutical-grade enteric polymer from Evonik Industries. PA6ACA, synthesized by a previously reported method[36], is structurally similar to traditional enteric polymers (for example, L 100-55, cellulose acetate succinate and hydroxyl propyl methyl cellulose phthalate). PA6ACA has side chains of sufficient length for the terminal carboxyl groups to be flexible and accessible, allowing the formation of intermolecular hydrogen bonds, as shown in Fig. 1a (ref. 36). In the acidic environment, where carboxyl groups are not deprotonated, inter-chain hydrogen bonds between carboxyl groups and amide units on PA6ACA and L 100-55 provide a loosely crosslinked supramolecular network with water trapped inside that contributes to the elastic property of the materials. In neutral or alkali aqueous environments, the carboxyl groups are deprotonated, eliminating the intermolecular hydrogen bonds, and resulting in rapid dissolution.

EEs with various compositions and properties were synthesized by co-precipitation of a solution of PA6ACA sodium salt and L 100-55 sodium salt in polymer weight ratios of 1:0, 1:1 and 1:2 with the addition of 6 M HCl solution, and then by compacting through ultracentrifugation (Fig. 1b, see Methods for details). The co-precipitation and ultracentrifugation process yielded macroscopically homogeneous materials with tough elastic properties and relatively low water contents (<35%, measurement method in Supplementary Information). Figure 1c shows a typical piece of EE taken from the ultracentrifuge tube (PA6ACA:L 100-55 1:2 shown here). EE could be easily cut into various shapes for the construction of devices or for mechanical characterizations. In preliminary mechanical testing (PA6ACA:L 100-55 1:2 as pictured in Fig. 1d), a cuboid shape that was pulled to three times its original length fully recovered its shape 5 min after the external force was removed, thus showing the desired elastic property in the absence of material fatigue.

Physical characterization of the EE

To better understand the structure–property relationship of EEs with various PA6ACA to L 100-55 ratios, we characterized the nanostructure, morphology, cytotoxicity, swelling, mechanical and enteric properties of these materials. At the molecular level, the hydrogen-bonding network of EEs was characterized by using small-angle X-ray scattering (SAXS) and infrared spectroscopy. The scattering profile of the PA6ACA gel (red curve in Fig. 2a) presents four broad peaks. Two peaks were found in the higher q-region, corresponding to periodic distances of around 3.1 Å and 2.3 Å. These were also found in pure water and thus can be

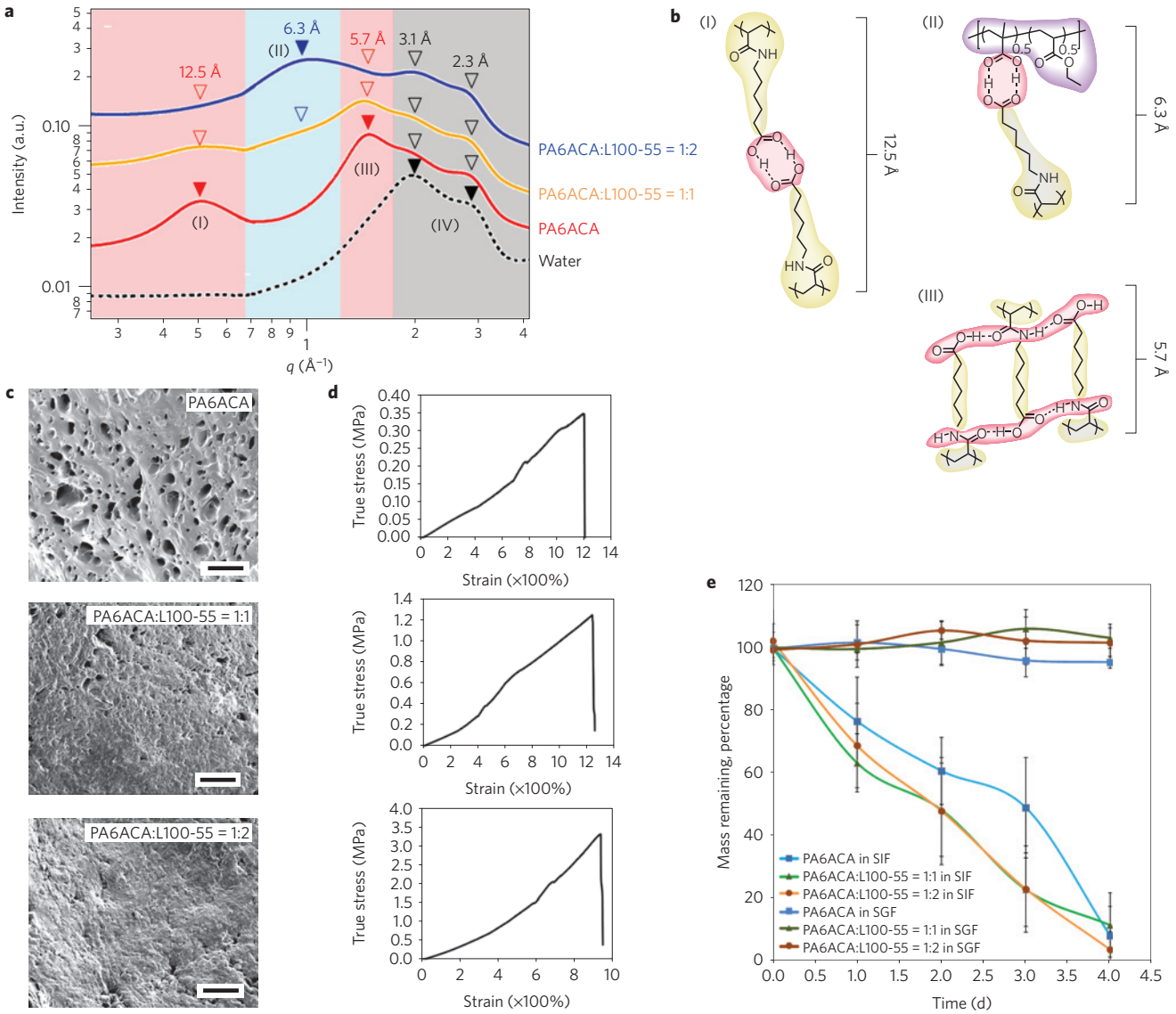

Figure 2 | Physical characterization of the enteric elastomer. a, SAXS data of EEs identified three major hydrogen-bonding structures (see main text for details). **b**, The carboxyl groups on PA6ACA interacting with the opposing carboxyl groups on PA6ACA in a face-on configuration (I), the carboxyl groups within PA6ACA interacting with the carboxyl groups on L 100-55 in a face-on configuration (II), and the carboxyl groups on PA6ACA interacting with amide groups of the opposing pendant side chain in an interleaved configuration (III). **c**, SEM images of dried polymer gels with various PA6ACA/L 100-55 weight ratios (top 1:0, middle 1:1, bottom 1:2). Scale bars, 50 μm. **d**, True stress–strain plots of polymer gels with PA6ACA/L 100-55 weight ratios (top 1:0, middle 1:1, bottom 1:2) stretched to breaking at 1 mm min^{-1}. **e**, Dissolution study of polymer gels in simulated gastric fluid (SGF) and simulated intestinal fluid (SIF) showing complete dissolution of the polymer gels in SIF for approximately four days, and no significant mass loss in SGF for the same period of time. EEs in ~1 cm^3 size were incubated in SGF and SIF at 37 °C, and then lyophilized. The mass remaining percentage equals the ratio of remaining dried weights to initial dried weights. The vertical error bars correspond to the standard deviations of a total of six samples per formulation.

attributed to hydrogen-bonding (defined as type IV) between H_2O molecules in the gel[37]. The other two peaks in the lower q-region of the SAXS profile represent two distinct periodic distances of 12.5 Å and 5.7 Å, which can be assigned to two coexisting hydrogen-bonding configurations between PA6ACA molecules in the gel: the face-on configuration (type I) and the interleaved configuration (type III), respectively (Fig. 2b). The formation of the two PA6ACA hydrogen-bonding configurations was further supported by infrared spectroscopy (Supplementary Fig. 1)[36]. When blending PA6ACA with L 100-55 in the gel, a new peak appears in the intermediate q-region (6.3 Å) of the SAXS profile, suggesting the formation of a new hydrogen-bonding configuration (type II, Fig. 2b) between PA6ACA and L 100-55. Increasing the content of L 100-55 in the polymer gels results in a relative increase in peak (II) with a reduction of peaks (I) and (III) in the SAXS profiles. Scanning electron microscopy (SEM) was employed to study the microstructure of EEs. As revealed by SEM images of lyophilized gels (Fig. 2c), three formulations of EE demonstrated porosity in the micrometre range, with a higher blending ratio of L 100-55 correlating with decreasing pore size. The water content decreased from 31.6 ± 3.8% in PA6ACA itself, to 27.7 ± 4.6% in the EE with ratio 1:1, and to 26.4 ± 3.5% in the EE with ratio 1:2, which is consistent with the SEM porosity findings.

We further tested the elastic and enteric properties, which are the two key functions of the EEs. The mechanical properties and the way in which these are influenced by the blending ratio of PA6ACA to L 100-55 were studied using an immersion tensile-stress tester in SGF at 37 °C. With increasing amount of L 100-55, the Young's

Figure 3 | Construction of a ring-shaped gastric-retentive device and *in vitro* testing of its elasticity and enteric property. a, Construction of a circle composed of polycaprolactone (PCL) arcs with intervening EE polymer gel linkers by first fitting cubic polymer gels and PCL beads alternately in a circle-shaped polydimethylsiloxane (PDMS) mould, followed by melting PCL at 70 °C. **b**, Folding of the ring into a standard gelatin 000 capsule by using the elasticity of the polymer gel. **c**, Escape from the capsule and recovery to the ring shape after dissolution of the gelatin capsule in SGF at 37 °C. **d**, Progressive dissolution of the EE supramolecular polymer gel linkers in SIF at 37 °C leads to for the dissociation of the circle-shaped device into PCL arcs.

modulus and tensile strength increased, and strain decreased. In the EE 1:1 formulation strain was noted at 1,207%, whereas in the 1:2 formulation it was observed at 943% (Fig. 2d). The stress–strain test suggests that the mechanical properties of EEs can be engineered by tuning the blending ratio of PA6ACA and L 100-55. The pH-dependent dissolution properties of EEs were evaluated in simulated gastric fluid (SGF, pH = ~1.2) and simulated intestinal fluid (SIF, pH = ~6.8). As shown in Fig. 2e, all three formulations of EEs showed long-term stability in SGF without detectable mass loss over four days. In contrast, within the same period of time, all three EEs were nearly dissolved in SIF in a pseudo-zero order manner with similar dissolution rates. To further modulate the enteric properties of EEs, we synthesized a copolymer of *N*-acryloyl 6-aminocaproic acid (A6ACA) and the more hydrophobic monomer *N*-acryloyl 11-aminoundecanoic acid (A11AUA), creating P(A6ACA$_{0.5}$-coA11AUA$_{0.5}$) (Supplementary Scheme S1, M_n = 82,300–170,600. M_w = 358,400–655,900). This copolymer was blended with L 100-55 at a weight ratio of 1:2, resulting in a material that completely dissolved in SIF in 18 days (Supplementary Fig. 2). Therefore, by modulating polymer-gel compositions through physical blending or chemical copolymerization, both the elastic and/or enteric properties of EEs could be adjusted.

To evaluate the biocompatibility and biosafety of EEs, EE sodium-salt forms were tested for their cytotoxicity towards multiple cell lines, including HeLa, HEK293 and the intestinal lines Caco-2 (C2BBe1 clone) and HT29-MTX-E12 (Supplementary Fig. 3). No significant cytotoxicity was observed for any of the three formulations of EEs over a wide range of concentrations from 0.078 to 20 mg ml^{-1} at the end of a 72 h incubation period. The observed cytotoxicity at very high concentrations (LD_{50} above 4.71 mg ml^{-1}) may be due to changes in pH or viscosity of the cell-culture medium after dissolving a large amount of high-molecular-weight polymer in sodium salts. EEs were further evaluated for swelling behaviour in several commonly ingested fluids, including vegetable oil and ethanol. EEs did not swell, and maintained their integrity in acidic aqueous solutions (pH $\leq$ 5.0) and in an acidic solution mixed with 10 wt% vegetable oil (see Supplementary Information). PA6ACA was evaluated for its ability to absorb ethanol. PA6ACA did not swell

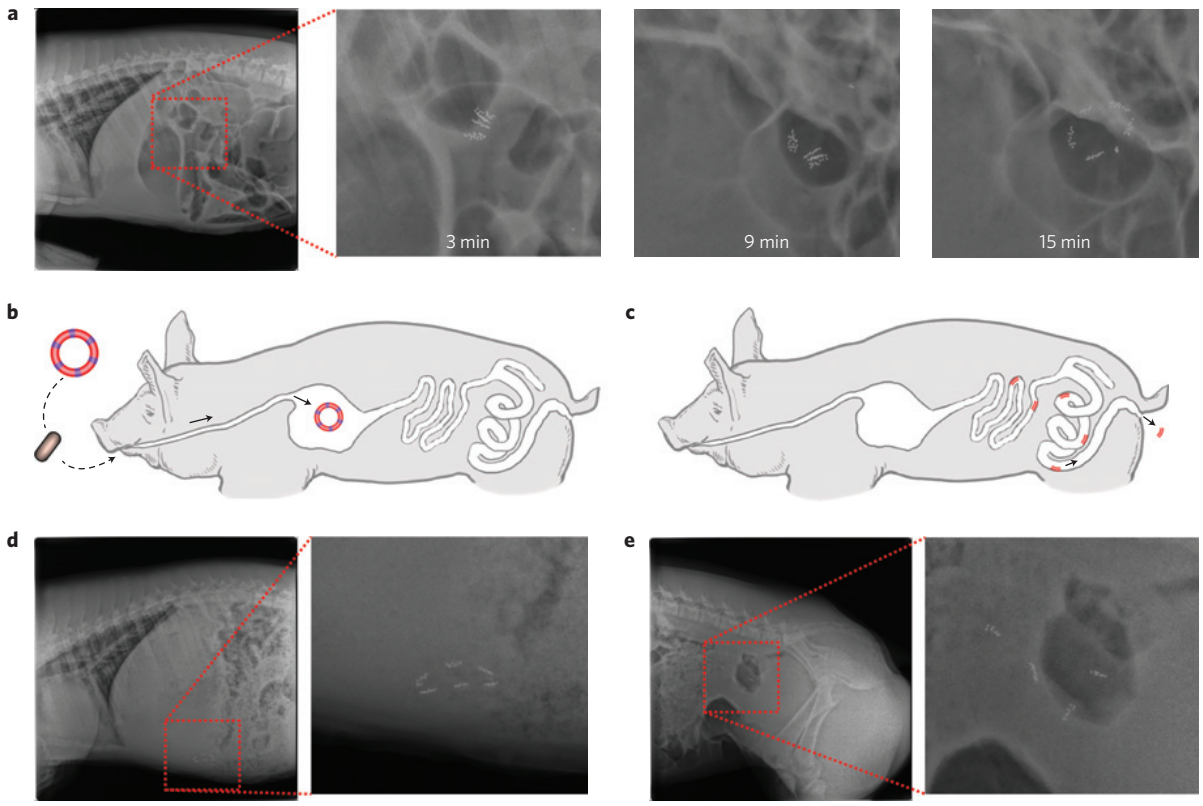

Figure 4 | *In vivo* evaluation of the ring-shaped devices in Yorkshire pigs. a, Recovery of the ring shape after delivery of an encapsulated ring-shaped device through the oesophagus and dissolution of the gelatin capsule in the stomach. **b**, Schematic representation of the delivery and gastric retention of a ring-shaped device. **c**, Schematic illustration of safe passage of PCL arcs through the small and large intestine on dissociation of the ring-shaped device as a result of the total or partial dissolution of EE linkers. **d**, X-ray image of a ring-shaped device residing in the gastric cavity of a Yorkshire pig. **e**, X-ray image of four PCL arcs passing through the intestine after dissolution of the EE linker. For visualization purposes, six to ten radio-opaque stainless steel beads (1 mm diameter) were incorporated in every PCL arm. The total bead mass was ~200 mg and the weight of the whole device (with iron beads) was ~1,000 mg.

noticeably in 10% ethanol (Supplementary Fig. 4), supporting the compatibility of this family of materials with common components of diets.

Fabrication and testing of gastric-retentive devices

As a step towards the goal of using EEs as key building blocks in gastric-retentive devices, we integrated EE and polycaprolactone (PCL) in prototype gastric-retentive devices. Owing to its high tensile strength, EE with PA6ACA/L 100-55 1:2 weight ratio was selected for the fabrication and testing of gastric devices in the rest of this study. For the structural component of the gastric devices we chose PCL, which is widely used as a biomaterial for implants and as a drug carrier owing to its proven biocompatibility, excellent mechanical properties and ease of manufacturing[38,39]. Generally, we first used a three-dimensional (3D) printer to generate positive moulds for the generation of negative polydimethylsiloxane (PDMS) moulds, then placed pieces of EE into the moulds and melted PCL at 70 °C to interface PCL with the EE for the formation of the integrated EE–PCL device. To assess the strength and integrity of the joint interface between EE and PCL, we placed EE in the centre of a dog-bone shaped device with PCL on both sides, and deformed the dog-bone by 180° as well as by linear extension until fracture. As shown in Supplementary Fig. 5, the EE has a low enough Young's modulus to tolerate 180° bending. During fracture testing, the EE-to-PCL interfaces remained intact, thus showing the stability of the interface and the feasibility of using PCL as a co-building block with EE for the fabrication of gastric-resident devices.

To demonstrate the utility of elastic and enteric functions of EE in gastric devices, we fabricated and tested a ring composed of PCL arcs with intervening EE linkers (Fig. 3). The maximal diameter of a device enabling gastric retention by preventing passage through the pylorus has been previously established as a key parameter[40–42]. Considering that the aperture diameter of the resting human pylorus is 12.8 ± 7.0 mm (ref. 14), we prepared a gastric-retentive device in a ring-shaped PDMS mould with an outer diameter of 32 mm, an inner diameter of 28 mm, a width of 2 mm and a depth of 2 mm. EE was cut into cuboid sections with the dimensions 6 mm × 4 mm × 2 mm, fitted in the moulds, and then dried by vacuum. This was followed by PCL placement and melting (Fig. 3a). As shown in Fig. 3b, the resulting ring-shaped device can be encapsulated by bending the elastic components up to 180° to fit into a standard 000 gelatin capsule. To simulate deployment and retention in the stomach environment, the encapsulated circle-shaped device was placed in SGF at 37 °C. The deployed device escaped from the capsule and recovered its original shape within 8 min (Fig. 3c). The medium was changed to SIF and the EE linkers slowly swelled and dissolved. As a result, the ring-shaped device gradually disassembled within 12 h (Fig. 3d). The elastic property of the EE enabled the encapsulation and restoration of the ring-shaped device following release from the capsule, whereas the enteric property allowed the dissociation of the device in SIF.

In vivo evaluation of gastric-resident devices

Having established *in vitro* the elastic and enteric properties imparted by the incorporation of the EE into prototypic devices, we next tested the *in vivo* application of gastric-retentive devices formed with EE, using a Yorkshire pig animal model. Yorkshire pigs weighing 45–55 kg have gastric and intestinal anatomy and

dimensions similar to humans, and have been previously used in the evaluation of other gastrointestinal devices[43]. Ring-shaped devices, as depicted in Fig. 3, were formed and encapsulated in 000 gelatin capsules with the addition of 1 mm stainless steel beads within the PCL arms for radiographic monitoring[12]. Under moderate sedation, the capsule was introduced through the oesophagus under endoscopic visualization. The encapsulated ring-shaped device deployed and restored its baseline shape in the stomach within 15 min (Fig. 4a). Four individual experiments on four different pigs were performed, demonstrating gastric retention of the device for two to five days (Fig. 4b,d). No intact devices were visualized outside of the stomach, suggesting that device breakage first occurred in the stomach. Loss of the intact device, that is, the partial dissolution and/or rupture of one or two EE linkers, which was visualized radiographically resulted in the linearization of the closed structure, thus enabling easier passage out of the stomach (Supplementary Fig. 6)[41]. On passage out of the stomach, the dissolvable EEs disintegrated, resulting in small rigid elements capable of safe passage without evidence of intestinal obstruction (Fig. 4c,e). Throughout the experiments the animals were found to have normal eating and stooling patterns and did not exhibit any signs of gastrointestinal obstruction, either clinically or radiographically. Radiographic visualization for the experiments above was enabled by the inclusion of radio-opaque beads in the PCL segments of the devices. To evaluate the possibility that the stainless steel beads in the PCL arms contributed to gastric retention, four encapsulated ring-shaped devices without iron beads were deployed into two pigs (two capsules per animal). Endoscopic imaging was used to evaluate the devices in the gastric cavity at the time points of 0.5 h, 2 days, 4 days and 7 days post deployment. All four rings were identified and were intact in the stomachs of the two animals after 0.5 h, 2 and 4 days, whereas only one ring was identified after 7 days (Supplementary Fig. 7). Gastric retention did not seem to be significantly affected by the elimination of the stainless steel beads, which represented ~20% of the total mass of the device.

The elastic function of the EE enabled the circle-shaped device to be folded into the standard 000 capsule for comfortable oral delivery, and also enabled shape recovery for prolonged gastric retention after dissolution of the capsule. The enteric function permitted the dissociation of the device into small pieces for safe passage through the lower gastrointestinal tract. This prototype device achieved extended gastric retention for two to seven days, as compared to the maximum of one to two days of gastric retention achieved by other reported gastric-retentive devices delivered by capsules[9,35].

Beyond the self-deployable gastric-retentive device delivered by capsules, we also explored exemplary gastric-resident devices for endoscopic delivery and placement (these included large devices composed similarly of PCL rigid segments linked together with EE and forming the letters 'M.I.T.)'. Those exemplary gastric-resident devices were constructed with EE and PCL, embedded with iron beads, and fabricated by using M-, I- and T-shaped PDMS moulds. These shapes could be folded and delivered through the oesophagus with endoscopic assistance. Radiographic images show elastic restoration of the M-, I- and T-shaped devices in three pig stomachs (Fig. 5b–d; left and middle) immediately after delivery. Endoscopic images also confirmed gastric retention of all three letters, and found no obstruction caused by those devices (Fig. 5b-d; right). All three M-, I- and T-shaped devices were retained in the gastric cavity for two to five days before their fragmentation (Supplementary Fig. 8). EEs can be used in the fabrication of a variety of gastric devices to prevent intestinal obstruction on exiting the stomach. The incorporation of dissolvable EE linkers enables the development of devices with potentially significantly improved safety profiles by allowing the fragmentation of the device into segments that can easily pass through the gastrointestinal tract. As demonstrated by the M.I.T.-shaped device, devices of significant size

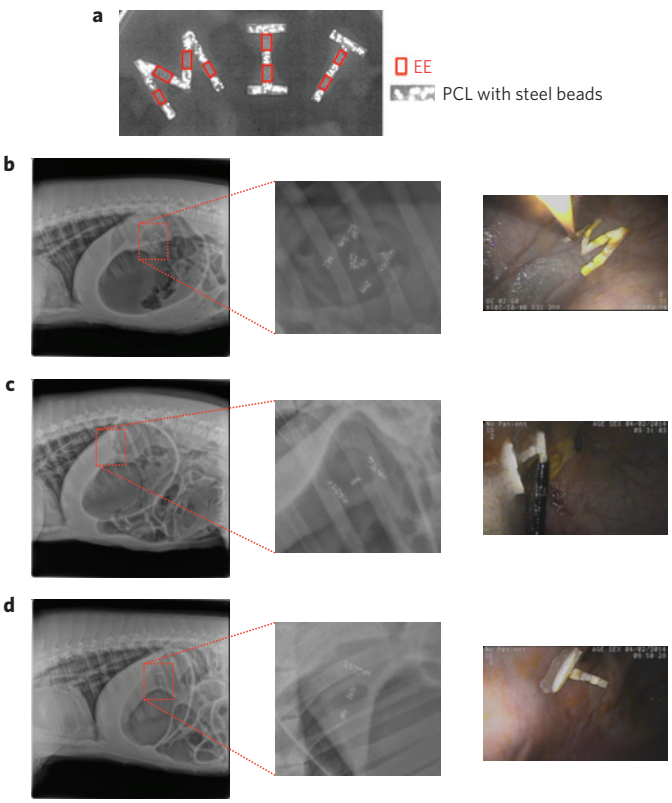

Figure 5 | *In vivo* evaluation of M-shaped (30 mm × 30 mm × 4 mm), I-shaped (30 mm × 18 mm × 4 mm) and T-shaped (30 mm × 18 mm × 4 mm) devices. a, X-ray image of M-, I-, and T-shaped devices made of EE as joints and PCL with embedded steel beads as X-ray contrast agent. **b**–**d**, X-ray images (left and middle) and endoscopic image (right) showing gastric retention of M-shaped (**b**), I-shaped (**c**) and T-shaped (**d**) devices.

can be safely deployed in the stomach, and can pass safely through the gastrointestinal tract on dissolution of the EEs. Restrictions on the size of gastric-resident devices hinge on the ability to deliver them to the gastrointestinal tract. In a conscious patient, the delivery of a device is limited by the size of the capsule or tablet that a patient is willing to swallow. Devices incorporating EEs and capable of safe fragmentation into small pieces could be introduced through endoscopic or minimally invasive access techniques, provided that they can pass through the oesophagus (in humans, ~2 cm in diameter). Supramolecular polymer gels with enteric and elastic properties could change the design and radically improve the adoption of novel gastric-resident devices for weight control, ingestible electronics and prolonged drug delivery.

Methods

Methods and any associated references are available in the online version of the paper.

Received 29 March 2015; accepted 17 June 2015;
published online 27 July 2015

References

1. Kethu, S. R. *et al.* Endoluminal bariatric techniques. *Gastrointest. Endosc.* **76,** 1–7 (2012).
2. Genco, A. *et al.* BioEnterics intragastric balloon: The Italian experience with 2,515 patients. *Obes. Surg.* **15,** 1161–1164 (2005).
3. Won, Y. W. *et al.* Oligopeptide complex for targeted non-viral gene delivery to adipocytes. *Nature Mater.* **13,** 1157–1164 (2014).
4. Tao, H. *et al.* Silk-based conformal, adhesive, edible food sensors. *Adv. Mater.* **24,** 1067–1072 (2012).

5. Kim, Y. J., Wu, W., Chun, S. E., Whitacre, J. F. & Bettinger, C. J. Biologically derived melanin electrodes in aqueous sodium-ion energy storage devices. *Proc. Natl Acad. Sci. USA* **110,** 20912–20917 (2013).
6. Byrne, C. & Lim, C. L. The ingestible telemetric body core temperature sensor: A review of validity and exercise applications. *Br. J. Sports. Med.* **41,** 126–133 (2007).
7. Belknap, R. *et al.* Feasibility of an ingestible sensor-based system for monitoring adherence to tuberculosis therapy. *PLoS ONE* **8,** e53373 (2013).
8. Moes, A. J. Gastroretentive dosage forms. *Crit. Rev. Ther. Drug* **10,** 143–195 (1993).
9. Hwang, S. J., Park, H. & Park, K. Gastric retentive drug-delivery systems. *Crit. Rev. Ther. Drug* **15,** 243–284 (1998).
10. Singh, B. N. & Kim, K. H. Floating drug delivery systems: An approach to oral controlled drug delivery via gastric retention. *J. Control Release* **63,** 235–259 (2000).
11. Fuhrmann, G. *et al.* Sustained gastrointestinal activity of dendronized polymer–enzyme conjugates. *Nature Chem.* **5,** 582–589 (2013).
12. Laulicht, B., Gidmark, N. J., Tripathi, A. & Mathiowitz, E. Localization of magnetic pills. *Proc. Natl Acad. Sci. USA* **108,** 2252–2257 (2011).
13. Salessiotis, N. Measurement of the diameter of the pylorus in man: Part I. Experimental project for clinical application. *Am. J. Surgery* **124,** 331–333 (1972).
14. Munk, J. F., Gannaway, R. M., Hoare, M. & Johnson, A. G. in *Gastrointestinal Motility in Health and Disease* (ed. Duthie, H. L.) Ch. 38, 349–359 (Springer, 1978).
15. Sultan, M. & Norton, R. Esophageal diameter and the treatment of achalasia. *Digest Dis. Sci.* **14,** 611–618 (1969).
16. Vanstiegmann, G., Cambre, T. & Sun, J. H. A new endoscopic elastic band ligating device. *Gastrointest. Endosc.* **32,** 230–233 (1986).
17. Dumonceau, J. M. Evidence-based review of the bioenterics intragastric balloon for weight loss. *Obes. Surg.* **18,** 1611–1617 (2008).
18. Cheifetz, A. S. *et al.* The risk of retention of the capsule endoscope in patients with known or suspected Crohn's disease. *Am. J. Gastroenterol.* **101,** 2218–2222 (2006).
19. McGovern, R., Barkin, J. S., Goldberg, R. I. & Phillips, R. S. Duodenal obstruction: A complication of percutaneous endoscopic gastrostomy tube migration. *Am. J. Gastroenterol.* **85,** 1037–1038 (1990).
20. Trande, P. *et al.* Efficacy, tolerance and safety of new intragastric air-filled balloon (Heliosphere BAG) for obesity: The experience of 17 cases. *Obes. Surg.* **20,** 1227–1230 (2010).
21. Roman, S. *et al.* Intragastric balloon for "non-morbid" obesity: A retrospective evaluation of tolerance and efficacy. *Obes. Surg.* **14,** 539–544 (2004).
22. Traverso, G. & Langer, R. Perspective: Special delivery for the gut. *Nature* **519,** S19 (2015).
23. Lappas, L. C. & Mckeehan, W. Synthetic polymers as potential enteric and sustained-release coatings. *J. Pharm. Sci.* **51,** 808 (1962).
24. Siepmann, F., Siepmann, J., Walther, M., MacRae, R. J. & Bodmeier, R. Polymer blends for controlled release coatings. *J. Control Release* **125,** 1–15 (2008).
25. Yan, X. Z., Wang, F., Zheng, B. & Huang, F. H. Stimuli-responsive supramolecular polymeric materials. *Chem. Soc. Rev.* **41,** 6042–6065 (2012).
26. Wojtecki, R. J., Meador, M. A. & Rowan, S. J. Using the dynamic bond to access macroscopically responsive structurally dynamic polymers. *Nature Mater.* **10,** 14–27 (2011).
27. Li, J. H., Viveros, J. A., Wrue, M. H. & Anthamatten, M. Shape-memory effects in polymer networks containing reversibly associating side-groups. *Adv. Mater.* **19,** 2851–2855 (2007).
28. Yan, X. Z. *et al.* A multiresponsive, shape-persistent, and elastic supramolecular polymer network gel constructed by orthogonal self-assembly. *Adv. Mater.* **24,** 362–369 (2012).
29. Jang, S. G., Kramer, E. J. & Hawker, C. J. Controlled supramolecular assembly of micelle-like gold nanoparticles in PS-b-P2VP diblock copolymers via hydrogen bonding. *J. Am. Chem. Soc.* **133,** 16986–16996 (2011).
30. Tee, B. C. K., Wang, C., Allen, R. & Bao, Z. N. An electrically and mechanically self-healing composite with pressure- and flexion-sensitive properties for electronic skin applications. *Nature Nanotech.* **7,** 825–832 (2012).
31. Chen, Y. L., Kushner, A. M., Williams, G. A. & Guan, Z. B. Multiphase design of autonomic self-healing thermoplastic elastomers. *Nature Chem.* **4,** 467–472 (2012).
32. Schaaf, P. & Schlenoff, J. B. Saloplastics: Processing compact polyelectrolyte complexes. *Adv. Mater.* **27,** 2420–2432 (2015).
33. Lendlein, A., Neffe, A. T. & Jérôme, C. Advanced functional polymers for medicine. *Adv. Healthc. Mater.* **3,** 1939–1940 (2014).
34. Stuart, M. A. C. *et al.* Emerging applications of stimuli-responsive polymer materials. *Nature Mater.* **9,** 101–113 (2010).
35. Sathish, D., Himabindu, S., Kumar, Y. S. & Shayeda Rao, Y. M. Floating drug delivery systems for prolonging gastric residence time: A review. *Curr. Drug Deliv.* **8,** 494–510 (2011).
36. Phadke, A. *et al.* Rapid self-healing hydrogels. *Proc. Natl Acad. Sci. USA* **109,** 4383–4388 (2012).
37. Luzar, A. & Chandler, D. Structure and hydrogen bond dynamics of water–dimethyl sulfoxide mixtures by computer simulations. *J. Chem. Phys.* **98,** 8160–8173 (1993).
38. Woodruff, M. A. & Hutmacher, D. W. The return of a forgotten polymer–polycaprolactone in the 21st century. *Prog. Polym. Sci.* **35,** 1217–1256 (2010).
39. Kearney, C. J. & Mooney, D. J. Macroscale delivery systems for molecular and cellular payloads. *Nature Mater.* **12,** 1004–1017 (2013).
40. Khosla, R. & Davis, S. S. The effect of tablet size on the gastric emptying of non-disintegrating tablets. *Int. J. Pharm.* **62,** R9–R11 (1990).
41. Cargill, R. *et al.* Controlled gastric emptying. 1. effects of physical properties on gastric residence times of nondisintegrating geometric shapes in beagle dogs. *Pharm. Res.* **5,** 533–536 (1988).
42. Martinez, M. N. & Papich, M. G. Factors influencing the gastric residence of dosage forms in dogs. *J. Pharm. Sci.* **98,** 844–860 (2009).
43. Swindle, M. M., Makin, A., Herron, A. J., Clubb, F. J. & Frazier, K. S. Swine as models in biomedical research and toxicology testing. *Vet. Pathol.* **49,** 344–356 (2012).

Acknowledgements

This work was funded in part by the Bill and Melinda Gates Foundation Grant OPP1096734 (to R.L.) and the NIH Grant EB000244 (to R.L.). The paper was partly sponsored by the Alexander von Humboldt Foundation under the auspices of the Max Planck Research Award to R.L. funded by the Federal Ministry of Education and Research. A.M.B. was supported in part by NIH T32 5T32HL007604-29. J.Z. was supported by the Laboratory Directed Research and Development program at Oak Ridge National Laboratory, which is sponsored by the Scientific User Facilities Division, Office of Basic Energy Sciences, US Department of Energy. Use of the Advanced Photon Source, an Office of Science User Facility operated for the US Department of Energy (DOE) Office of Science by Argonne National Laboratory, was supported by the US DOE under Contract No. DE-AC02-06CH11357. We would like to thank J. Haupt and M. Jamiel for expert veterinary support. We are indebted to L. Wood, P. Eckhoff, D. Hartman, S. Kern, S. Hershenson and B. Nikolic for fruitful discussions that stimulated the development of this material. The findings and conclusions reported in this paper are those of the authors and do not necessarily reflect positions or policies of the Bill and Melinda Gates Foundation.

Author contributions

S.Z., R.L. and G.T. designed the material and experiments. S.Z. prepared the material and the device. S.Z., A.M.B., D.L.G., R.B., Y.-A.L.L., J.Z., V.A.M., C.C., L.D.N., D.J.M., L.G. and G.T. characterized the material, analysed the data and wrote the paper. R.L. and G.T. supervised the research. All authors discussed the progress of research and reviewed the manuscript.

Additional information

Supplementary information is available in the online version of the paper. Reprints and permissions information is available online at www.nature.com/reprints. Correspondence and requests for materials should be addressed to R.L. or G.T.

Competing financial interests

The authors declare Provisional US patent application No. 62/010,992 filed on 11 June 2014.

Methods

Materials. 6-Aminocaproic acid, 11-aminoundecanoic acid, NaOH, hydrochloric acid (ACS reagent, 37%), NaCl, tetramethylethylenediamine, ammonium persulphate, polycaprolactone (PCL, average M_n 80,000) and KH_2PO_4 were used as received from Sigma-Aldrich Company (St. Louis). Acryloyl chloride was purchased from Sigma and vacuum distilled before use. Nanopure water (18 MΩ cm) was acquired by means of a Milli-Q water filtration system, Millipore (St. Charles). 1 l of simulated gastric fluid (SGF, pH ∼ 1.2) was made by dissolving 2 g NaCl and 8.3 ml concentrated HCl in water and adjusting to 1,000 ml with water. 1 l of simulated intestinal fluid (SGF, pH ∼ 6.8) was made by dissolving 6.8 g KH_2PO_4 and 0.896 g NaOH in water and adjusting to 1,000 ml with water.

Synthesis of PA6ACA sodium salt. To a nitrogen-bubbled solution containing 10 g (54.1 mmol) A6ACA, 2.16 g (54.1 mmol) NaOH and 6.3 mg (0.0541 mmol) tetramethylethylenediamine (TMEDA) dissolved in 400 ml nanopure water at 40 °C was added a solution of 62 mg (0.270 mmol) ammonium persulphate in 10 ml nanopure water. The reaction mixture was allowed to stir for 12 h for the polymerization. The polymer solution was transferred to dialysis tubes (MWCO 3500 Da) for dialysis for three days and lyophilized, obtaining a white solid powder with an average yield of 95%. ^{1}H NMR (D_2O, ppm): δ 3.15 (s, CONHCH_2CH$_2$), 2.20 (d, CH2CH$_2$CH_2COO–), 2.02 (b, CONHCH$_2$CH$_2$), 1.57 (s, CH$_2$CH_2CH$_2$COO–), 1.55 (s, CONHCH$_2$CH_2), 1.33 (s, CH_2CH$_2$CH$_2$COO–), 1.70-1.25 (b, CH_2CHCO). ^{13}C NMR (D_2O, ppm): δ 183.52, 176.13, 39.56, 37.42, 28.33, 28.26, 26.31, 25.51. M_n = 61,600–112,700. M_w = 347,300–466,300. IR: 3,600–3,000, 2,911, 2,843, 1,638, 1,536, 1,395, 1,302, 1,210, 1,165, 1,099 cm^{-1}. DSC: (T_g) = 94.2 °C.

Synthesis of P(A6ACA$_{0.5}$-co-A11AUA$_{0.5}$) sodium salt. To a nitrogen-bubbled solution containing 10 g (39.2 mmol) A11AUA, 7.25 g (39.2 mmol) A6ACA, 3.14 g (78.4 mmol) NaOH and 9.1 mg (0.0784 mmol) tetramethylethylenediamine (TMEDA) in 700 ml nanopure water at 40 °C was added a solution of 89 mg (0.392 mmol) ammonium persulphate in 10 ml nanopure water. The reaction mixture was allowed to stir for 12 h for the polymerization. The polymer solution was transferred to dialysis tubes (MWCO 3500 Da) for dialysis for three days and lyophilized, obtaining a white solid powder with an average yield of 87%. ^{1}H NMR (D_2O, ppm): δ 3.14 (s, CONHCH_2CH$_2$), 2.21 (s, CH$_2$CH$_2$CH_2COO–), 1.99 (s, b, CONHCH$_2$CH$_2$), 1.59 (s, CH$_2$CH_2CH$_2$COO–), 1.52 (s, CONHCH$_2$CH_2), 1.33 (s, CH_2CH$_2$CH$_2$COO–), 1.70–1.25 (b, CH_2CH_2CH_2CH_2CH_2CH_2CH$_2$ CH$_2$COO–, CH_2CHCO). ^{13}C NMR (D_2O, ppm): δ 183.57, 176.09, 39.58, 37.74, 37.54, 28.99, 28.29, 26.87, 26.33, 26.08, 25.85, 25.57. M_n = 82,300–170,600. M_w = 358,400–655,900. IR: 3,500–3,000, 2,912, 2,843, 1,642, 1,552, 1,402, 1,302, 1,101 cm^{-1}. DSC: (T_g) = 97.6 °C. A 50:50 composition ratio of P(A6ACA$_{0.5}$-co-A11AUA$_{0.5}$) was the feeding ratio of the radical polymerization. A 50:50 feeding ratio should be very close to the actual composition ratio of the resulting copolymer, based on the nearly quantitative conversion of two monomers after the polymerization.

Preparation of enteric elastic polymer gels with various compositions. To a well-mixed solution containing 1 g PA6ACA sodium salt, 0.853 g of poly(methacrylic acid-co-ethyl acrylate) (EUDRAGIT L 100-55) and 0.183 g NaOH dissolved in 45 ml nanopure water, a solution of 5 ml of 6 M HCl (diluted from ACS grade concentrated 37% HCl) was quickly added. The mixture was put on the vortex shaker for 5 min, then transferred into thick-wall centrifuge tubes (Beckman Coulter) and centrifuged in a Beckman Coulter Ultracentrifuge (Avanti J-26 XP) using an SW 32 Ti rotor at 32,000 r.p.m. for 2 h at 20 °C. The resulting enteric elastic polymer gels with PA6ACA/L 100-55 ratio 1:1 were extracted from the bottom of the ultracentrifuge tube.

Nuclear magnetic resonance (NMR) characterization. ^{1}H NMR and ^{13}C NMR spectra were recorded on a VARIAN Mercury 300 NMR Spectrometer with an Oxford Instruments superconducting magnet—A 300 MHz NMR spectrometer interfaced to a UNIX computer using VNMR 6.1c software. Chemical shifts were referenced to the solvent resonance signals.

Gel permeation chromatography. Aqueous gel permeation chromatography (GPC) was conducted on a Viscotek system (Malvern) equipped with an isocratic pump Viscotek VE 1122 solvent delivery system, TDA 305 triple detector array, and 3× TSK Gel GMPWxL column with guard column. The system was equilibrated at 30 °C in pre-filtered water containing 0.05 M $NaNO_3$ with the flow rate set to 1.00 ml min^{-1}. Polymer solutions were prepared at a concentration of about 1–3 mg ml^{-1} and an injection volume of 200 µl was used. Data collection and analysis were performed with ChemStation for LC (Agilent) and OmniSEC v. 4,6,1,354 software (Malvern). The system was calibrated with poly(ethylene oxide) standards (Sigma) ranging from 400 to 511,000 Da (M_p). The charged synthetic polymers in this manuscript may interact with the GPC column even when the salt eluent is used, therefore the GPC molecular weights based on uncharged PEO standards may be an underestimate[44].

Infrared spectroscopy. Infrared spectra were recorded on an ALPHA FT-IR Spectrometer (Bruker) and analysed using OPUS v. 6,5,92 software.

Differential scanning calorimetry (DSC). Glass transition temperatures (T_g) were measured by differential scanning calorimetry on a PerkinElmer DSC 8000 (PerkinElmer), with heating and cooling rates of 5 °C min^{-1} in the range between −50 °C and 150 °C under a nitrogen atmosphere. Measurements were analysed using Pyris v 11.0.0.0449 software. The T_g was taken as the midpoint of the inflection tangent, on the third heating scan of three heating/cooling cycles.

Water content measurement and SEM analysis. Three formulations were dried by lyophilization for 48 h to measure their water content. The morphology of lyophilized polymer gels was analysed by means of a Zeiss Ultra55 field-emission scanning electron microscope after being carbon coated.

Small-angle X-ray scattering (SAXS). SAXS experiments were conducted by the DuPont–Northwestern–Dow Collaborative Access Team (DND-CAT) of the Advanced Photon Source at Argonne National Laboratory. X-rays of wavelength λ = 0.73 Å were used and each measurement was performed at room temperature using three different sample-to-detector distances (0.2, 1.0 and 7.5 m) to cover an q-range of $0.0026 < q < 4.4$ Å^{-1}, where $q = (4\pi/\lambda)\sin(\theta/2)$ is the magnitude of the scattering vector and θ is the scattering angle. Our gel samples were prepared into a disk shape and fixed vertically to have the X-ray beam pass through the centre of the wet samples. Samples were approximately 1.0 mm thick and 3.0 cm in diameter.

Immersion tensile testing. An MTS Synergie 400 Tensile Test Machine equipped with a circulating and heating Bionix Mini Bath and an electronic temperature probe was used for the immersion tensile testing. For testing, EEs were cut in approximately 2 mm × 2 mm × 20 mm pieces, and held by wedge action grips, exposing 6–12 mm for the testing. SGF at 37 °C was added into the bath and EEs were allowed to equilibrate in SGF for 10 min before pulling. The stretch rate was set to 10 mm min^{-1}. EEs were submerged in SGF during the whole testing process until the fracture.

Dissolution studies. EEs were cut into ∼1 cm^3 sized cubes and submerged in either 40 ml SGF or SIF in a 50 ml VWR centrifuge tube. Six replicates for each time point and condition were incubated at 37 °C on a shaker plate at 250 r.p.m. The solutions were exchanged with fresh SGF or SIF every 12 h. At each time point, cubes were lyophilized for 48 h before weighing. The remaining mass percentage equals the ratio of remaining dried weight to initial dried weight.

Swelling tests. Pre-weighted EEs cubes (∼1 cm^3) were submerged in either 40 ml SGF blending with certain ratio of vegetable oil (10%) or ethanol (10–50%) in a 50 ml VWR centrifuge tube. Three replicates for each solvent condition were incubated at 37 °C on a shaker plate at 250 r.p.m. After 24 h, samples were weighed and compared with initial weights. For SGF with 10% vegetable oil, EE did not gain detectable weight. For SGF with ethanol, swelling data is shown in Supplementary Fig. 4.

Cytotoxicity study. PA6ACA sodium salt and L 100-55 were dissolved in an aqueous NaOH solution. Subsequently the pH was adjusted to 7.0 using 1 M HCl. The final polymer solution was diluted with Dulbecco's Modified Eagle Medium (DMEM) (Life Technologies) to 100 mg ml^{-1} before testing. Cytotoxicity was tested on HeLa, HEK293, C2BBe1 (ATCC) and HT29-MTX-E12 cells (Public Health England) by seeding them in a 96-well plate at a densities of 6 × 103, 16 × 103, 16 × 103 and 2 × 104 cells/well respectively. Cell lines were freshly purchased from ATCC and Public Health England for these experiments. To avoid cross contamination, expanded cells were stored in individual containers. Regular mycoplasma evaluations were performed of the cell culure environment to ensure the absence of mycoplasma contamination. Individual cell lines were not evaluated for mycoplasma. HeLa and HEK293 cells were cultured in 100 µl DMEM containing 1% non-essential amino acids, 10% fetal bovine serum (FBS) and 1% penicillin–streptomycin solution (Life Technologies) per well. C2BBe1 and HT29-MTX-E12 cells were cultured in the same medium, but were additionally supplemented with 4 mg ml^{-1} human transferrin (Life Technologies). Cells were kept in culture for three days before replacing the medium, to which the dissolved aqueous polymer solutions were added (final concentrations of polymers ranged from 0.078 to 20 mg ml^{-1}). After 72 h, cytotoxicity was quantified by adding 10 µl alamarBlue reagent (Life Technologies) to each well. The contents were mixed well and then allowed to incubate at 37 °C for 1 h. Absorbance at 570 nm was recorded on an Infinite M200Pro (Tecan) using 600 nm as the reference wavelength. A positive control was provided by lysing cells with 1% Tween-20; cells that were not subject to any polymer provided a negative control. Cell viability was calculated by

the following equation: Cell viability (%) = 100 × (Absorbance(sample) − Absorbance(positive control))/(Absorbance(negative control) − Absorbance(positive control)).

Construction of gastric-retentive devices bearing EE and polycaprolactone (PCL). An Objet 3D printer using DurusWhite RGD430 build material and Support Fullcure 705 as support material was used to generate shapes as positive models. Negative moulds were created by casting polydimethylsiloxane (PDMS) (SYLGARD 184 Silicone Elastomer Kit, Dow Corning) around positive models. EE (PA6ACA/L 100-55 1:2 ratio) was cut into cubes or cuboids to fit into the PDMS moulds and dried by vacuum. Beads of PCL (Sigma, M_n 80k) were placed between EE pieces in the PDMS moulds and melted at 70 °C for 12 h before cooling to room temperature. Resulting devices bearing EE and PCL were submerged in SGF for two days to completely hydrate EE before devices were removed from the moulds.

Pig large animal model. All procedures were conducted in accordance with protocols approved by the Massachusetts Institute of Technology Committee on Animal Care. Six separate female Yorkshire pigs weighing approximately 45–55 kg were used for *in vivo* evaluation. Before the procedures the animals were fasted overnight. On the day of the procedure, the morning feed was held and the animals were sedated with Telazol (tiletamine/zolazepam) 5 mg kg^{-1}, xylazine 2 mg kg^{-1} and atropine 0.04 mg kg^{-1}. To ensure gastric placement of the devices the devices were placed in the stomach with the use of an oesophageal overtube (US Endoscopy) which was placed endoscopically in the oesophagus. Radiographs were performed every 48–72 h to monitor the integrity and transit of the devices as well as any radiographic evidence of bowel obstruction or perforation. Furthermore, all animals were monitored clinically at least twice a day for any evidence of obstruction, including poor feeding, poor defecation, abdominal distension and vomiting. Where radio-opaque fiducials were omitted from prototype devices, visualization was performed endoscopically.

References

44. Cooper, A. R. & Matzinger, D. P. Aqueous gel permeation chromatography: The effect of solvent ionic strength. *J. Appl. Polym. Sci.* **23,** 419–427 (1979).